Electronic Supplementary Material (ESI) for Journal of Materials Chemistry C.
This journal is © The Royal Society of Chemistry 2017

Supporting information

Macroscopically Aligned Nanowire Arrays of π-Conjugated Polymers *via* Shear-Enhanced Crystallization

Jun-Huan Li, [a,b] Yuyin Xi, [c] Lilo D. Pozzo, [c] Jun-Ting Xu *[a] and Christine K. Luscombe *[b,d]

[a]MOE Key Laboratory of Macromolecular Synthesis and Functionalization, Department of Polymer Science & Engineering, Zhejiang University, Hangzhou 310027, China

[b]Materials Science & Engineering Department, University of Washington, Seattle, Washington 98195-2120, United States

[c]Department of Chemical Engineering, University of Washington, Seattle, Washington 98195-1750, United States

[d]Department of Chemistry, University of Washington, Seattle, Washington 98195-1700, United States

Experimental details 2

Description of HSPs 3

^{1}H NMR and SEC spectra of LM-P3HT sample 4

TEM images of P3HT films 5

^{1}H NMR and SEC spectra of HM-P3HT sample 7

1D diffraction profile of GISAXS 8

Mobility distribution of OFETs 8

Reference 9

Experimental details

Materials

Regioregular poly(3-hexylthiophene)s (P3HTs) with a low molecular weight (M_n = 6.0×10^3 g/mol, $Đ$ = 1.14, regioregularity (RR)% = 97%) and a high molecular weight (M_n = 2.0×10^4 g/mol, $Đ$ = 1.22, RR% = 98%), hereafter marked as LM-P3HT and HM-P3HT, respectively, were synthesized *via* the GRIM method.[1] Commercial product P3HT (RMI-001EE, M_n = 3.2×10^4 g/mol, $Đ$ = 1.74) was purchased from Rieke Metals Inc. Ethyl benzoate (EB), chlorobenzene (CB) and 1,2,4-trichlorobenzene (TCB) were purchased from Sigma-Aldrich.

Preparation of P3HT thin films:

P3HT (3 mg) was dissolved in a solvent (10 mL) and heated at 85 ºC for 30 min. LM-P3HT was dissolved in EB while HM-P3HT was dissolved in EB/TCB mixture with a volume ratio of 2:1. The solution was then cooled to a lower temperature (45, 35 or 25 °C) and left unperturbed for 10 min after which it was filtered through the PTFE filter (0.2 µm). The filtrate (30 µL) was drop cast onto a cleaned silicon substrate which was placed beside a filter paper (1.5 cm × 1.5 cm) with a common contact area in petri dish beforehand to absorb the excess solution and preserve only a thin liquid membrane on the substrate. Prior to drop casting, the silicon substrate was cleaned by ultrasonication in deionized water, acetone, and isopropyl alcohol for 10 min each, and then dried under N_2 flow. Next, the silicon substrate was placed in air plasma cleaner for 10 min prior to drop casting. The petri dish was then covered with a lid and kept undisturbed overnight to allow the solvent to fully volatize. In the case of using an inclined substrate, the substrate was inclined to a certain angle as measured using a goniometer. The P3HT solution (0.3 mg/mL) and the samples were prepared at room temperature (25 ºC) on the inclined substrate at 30º angle. For the spin-coated samples, P3HT (3 mg) was dissolved in 1 mL solvent to prepare P3HT thin films with ca. 30 nm thickness similar to the films made by substrate-inclined method. The solution was heated at 85 ºC for 30 min. Then the solution was cooled down to room temperature (25 ºC) and filtered through the PTFE filter (0.2 µm). The prepared solution was spin coated at 1000 rpm onto the cleaned substrates for 2 min.

Characterization

Transmission electron microscopy (TEM) observations were performed on a JEOL JEM-1230 electron microscope at an acceleration voltage of 80 kV. The samples for TEM were prepared by dropping the prepared solution (10 µL) onto the carbon-coated copper grid. A filter paper was placed beside the copper grid to absorb the excessive solution and preserve only a thin liquid membrane on the copper grid. The petri dish was then covered with a lid and kept undisturbed to allow the solvent volatize slowly. The number-average molecular weight (M_n) and molecular weight distribution (M_w/M_n) of P3HT were determined by *size exclusion chromatography (SEC)* on a PL-220 SEC instrument with tetrahydrofuran as the eluent at 40 °C and a flow rate of 1 mL/min, using a poly(styrene) standard from Waters Corp. *^{1}H NMR* spectra were recorded at room temperature using a Bruker (400 MHz) spectrometer using tetramethylsilane as the internal standard and $CDCl_3$ as the solvent. *Polarized UV-vis* data were obtained in transmission geometry using Carry 500 spectrometer. The spectral resolution was 1 nm and the incident light was polarized parallel and perpendicular to the substrate-shearing direction for each measurement of oriented nanowire array films deposited on the inclined glass substrate. *Atomic Force Microscopy (AFM)* studies were conducted in PeakForce mode using a Dimension Icon, (Bruker Santa Barbara, USA). ScanAsyst-air probes with ca. 10 nm tip radii, purchased from Bruker were used to obtain all images. *Thickness measurements* were performed on a Bruker Dimension 3100 by scratching the samples with a razor blade. Bruker OTESPA probes were used for all thickness measurements (resonant frequency ~300 kHz and spring constant ~40 N/m). Imaging was conducted in air at ambient temperature. Images were analyzed using Gwyddion software. An Olympus BX51-P microscope with cross-polarizer was used to record optical micrographs of the polymer films deposited on cleaned silicon substrates. *Grazing-incidence small angle x-ray scattering (GISAXS)* characterizations were performed on Anton Paar SAXSess instrument. A wavelength of 1.54 Å X-ray was generated by Cu Kα tube. The samples were prepared either by shear alignment or spin coating on SiO_2 substrates with a dimension of 1.5 by 1.5 cm^2. An automated stage was utilized to align the tilt angle of the substrate to be 0.2º relative to the incident beam. The 2-D scattering pattern was collected by image plates after counting for 15 h. Distorted Wave Born Approximation (DWBA) was implemented in order to treat the polymer scattering analytically. Customized Igor Pro macros were programmed to convert the raw images with respect to sample reference frame. The intensity was normalized to the total scattering time.[2]

Fabrication of devices:

Organic field-effect transistors (OFETs) were fabricated in a top-contact bottom-gate device geometry on heavily doped p-type silicon ⟨100⟩ wafers with a 300 nm thermal oxide layer, purchased from WRS Materials Silicon Supplier and Service Company. Substrates were cleaned by sequential ultrasonication with acetone, methanol, and isopropyl alcohol for 15 min each. They were then dried under a stream of nitrogen and treated by UV-Ozone for 10 min. Solutions of P3HT were used as prepared for P3HT thin film experiments and drop casted or spin coated onto the silicon substrates and placed in the air overnight to allow any remaining solvent to evaporate. Gold source and drain electrodes were thermally evaporated through a shadow mask at a base pressure of 5×10^{-7} Torr at a rate of 1 Å/s to a thickness of 50 nm. The output and transfer characteristics of all transistors were measured in a nitrogen atmosphere using a standard four-probe setup with an Agilent 4155B semiconductor parameter analyzer. All devices had channel lengths of 100 μm and channel widths of 1000 μm. At least five substrates and 15 devices were tested for each processing condition. The saturated charge carrier mobility for each polymer film was calculated using the saturation current equation (Eq S1):

$$I_{ds} = \mu \cdot W \cdot C_0 \cdot (V_g - V_t)^2/2L \qquad \text{Eq S1}$$

Where I_{ds} is the drain-source current; μ is the field-effect mobility; W is the channel width (1000 μm); L is the channel length (100 μm); C_0 is the capacitance per unit area of the insulator (SiO_2, 300 nm, 10 nF·cm^{-2}); V_g is the gate voltage; and V_t is the threshold voltage.

Description of HSPs

The solubility parameter (δ) is defined as the square root of the cohesive energy density (E_C) over the molar volume of the pure material (V):[3]

$$\delta = (E_C \,/\, V)^{\frac{1}{2}} \qquad \text{Eq S2}$$

The total cohesive energy is divided into three components; E_D, E_P and E_H which describe the energy involved in three principle types of interactions, namely, dispersion interactions, dipolar-dipolar molecular interactions, and hydrogen bonding interactions. Therefore, the parameter δ is similarly substituted by three components that describe these three interactions:

$$E_C = E_D + E_P + E_H \qquad \text{Eq S3}$$

$$\delta^2 = \delta_D^2 + \delta_P^2 + \delta_H^2 \qquad \text{Eq S4}$$

Where δ_D, δ_P and δ_H are the Hansen solubility parameters (HSPs). Graphically, every chemical compound can be represented by its position in a 3D space, the Hansen solubility space, with coordinates defined by the three solubility parameters. The solubility of a solute in a solvent is predicted from similarities in their HSPs. Such similarity is quantified by the distance R_A between the HSPs of the solvent and the solute. The distance R_A is calculated using the following equation:

$$R_A^2 = \mathrm{a}(\delta_{D1} - \delta_{D2})^2 + b(\delta_{P1} - \delta_{P2})^2 + c(\delta_{H1} - \delta_{H2})^2 \qquad \text{Eq S5}$$

Subscripts 1 and 2 represent the solvent and solute, respectively. Setting of a = 4 and b = c = 1 was suggested by Hansen based on empirical testing.[4] The solute is described as a sphere in the Hansen solubility space, in which the HSPs are the center of the sphere and R_O is the radius representing the boundary of solubility. The interactions between a solvent and a solute are considered to be strong only if the distance R_A is smaller than the radius of the sphere R_O. Here the relative energy difference (*RED*) is provided as a numerical parameter to compare R_A and R_O, and is defined as:

$$RED = R_A/R_O \qquad \text{Eq S6}$$

The *RED* provides an estimate of whether two materials are miscible. If the *RED* is higher than 1, the solvent is outside the solubility sphere of the solute and can be expected to be a bad solvent. On the other hand, if the *RED* is between 0 and 1, the solvent is inside the solubility sphere of the solute and is expected to be a good solvent. As shown in Table S1 and Fig. S1, both CB and TCB are good solvent of P3HT and inside the solubility sphere of P3HT while EB is a relatively poor solvent of P3HT and close to the border of the solubility sphere of P3HT.[5-7]

Table S1. HSPs of P3HT and selected solvents[5-7]

Materials	δ_D (MPa$^{1/2}$)	δ_P (MPa$^{1/2}$)	δ_H (MPa$^{1/2}$)	R[a]	*RED*
P3HT[b]	19.45	3.97	4.19	4.30	-
CB	19.00	4.30	2.00	2.39	0.56
TCB	20.20	6.00	3.20	2.71	0.63
EB	17.90	6.20	6.00	4.22	0.98

[a] R refers to R_O for P3HT and R_A for solvents. [b] The P3HT has a M_n of 4.03 ×10^4 and $Đ$ of 2.27.

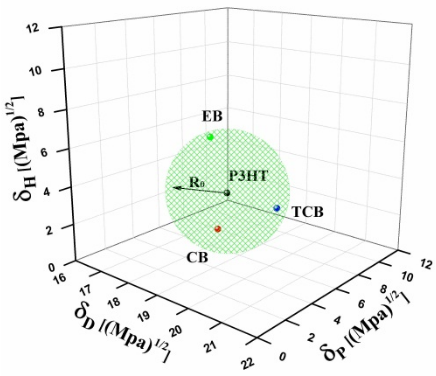

Fig. S1. HSP diagrams for P3HT and selected solvents.

^{1}H NMR and SEC spectra of LM-P3HT sample

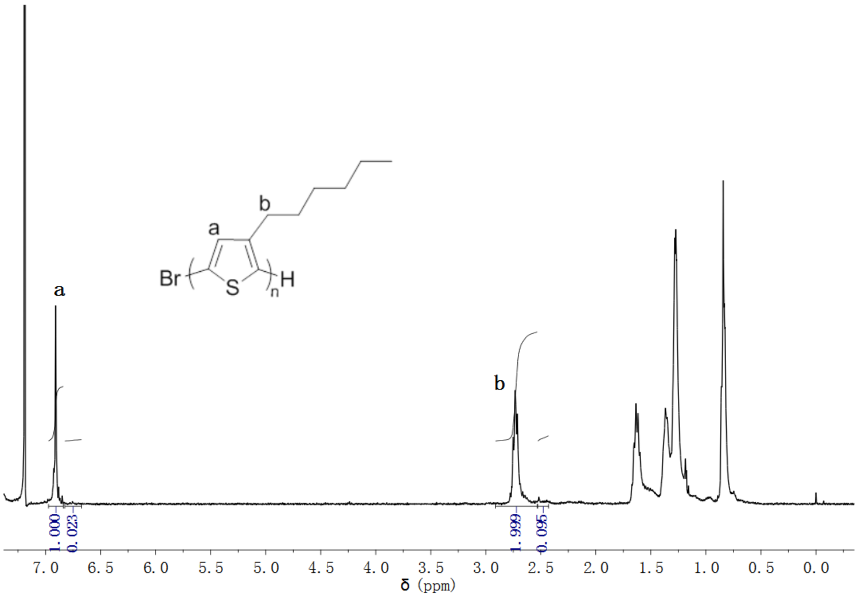

Fig. S2 ^{1}H NMR spectrum of LM-P3HT.

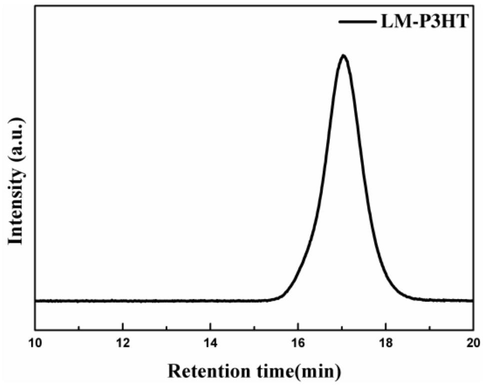

Fig. S3 Size exclusion chromatogram of LM-P3HT.

TEM images of P3HT films

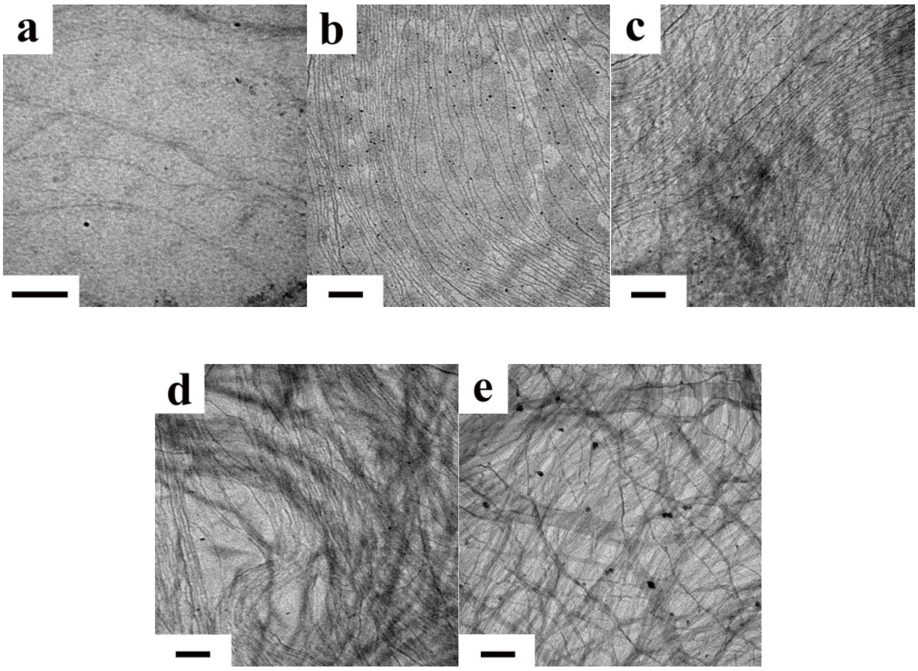

Fig. S4 TEM images of films made by depositing equal volume (10 µL) of EB solution of LM-P3HT on the horizontal substrate with concentrations of (a) 0.1, (b) 0.3, (c) 0.5, (d) 0.7 and (e) 1.0 mg/mL at 25 ºC, respectively. Scale bar = 200 nm.

The concentration of P3HT in solution has a great impact on the formation of the crystalline nanowires.[8] Under low-concentrations, where there are insufficient molecules, the nanowires grew randomly and only partially covered the substrate (Fig. S4a) because of the limited interaction between the loose nanowires. When the concentration reached an appropriate value (about 0.3 mg/mL), the presence of an adequate number of molecules ensured the continuous crystallization for nanowire growth (Fig. S4b). Furthermore, the interaction between the adjacent nanowires would favor the parallel growth along the same direction. However, when the concentration was too high (Fig. S4d and S4e), the nanoribbon, a different crystalline aggregate, was formed in the interior area of the liquid membrane, while the compact nanowires were formed as the air-liquid-solid interface gradually retreated. So the nanowires would then spread above the nanoribbons which affected the arrangement of the nanowires adversely, resulting in the disordered packing of multilayers.

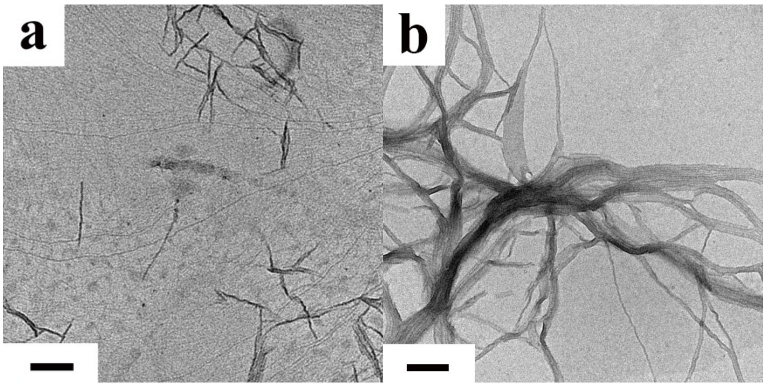

Fig. S5 TEM images of films made by depositing equal volume (10 µL) of EB solution of LM-P3HT (0.3 mg/mL) on the horizontal substrate at temperatures of (a) 35 ºC and (b) 45 ºC. Scale bar = 200 nm.

The temperature of both the solution and the substrate also affects the crystallization of P3HT.[9] When the temperature of the solution and substrate was increased, the formation of nanowire arrays was suppressed and replaced by short nanowire aggregates and then nanoribbons (Fig. S5b). Since the higher temperature contributes to better solubility of P3HT, the polymers chains would be able to move to the interior area rather than separate out from the solution and stack into ordered nanowires at the air-liquid-solid interface as the solvent evaporates. In other words, the role of the directional retreating of the three-phase interface on nanowire alignment became ineffective. In addition, the higher temperature accelerated the evaporation of the solvent, which reduced the time available for the growth of crystalline nanowires.

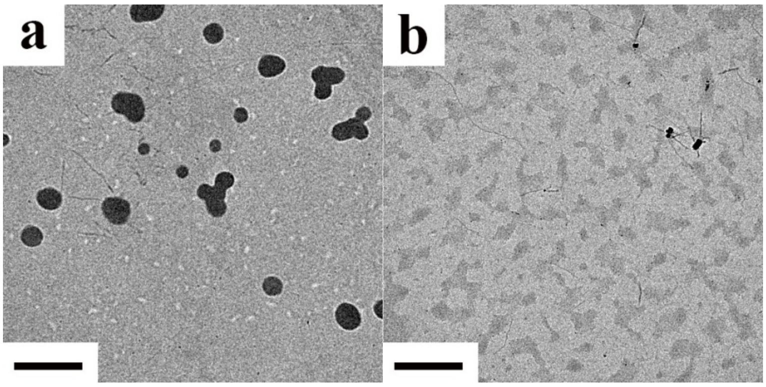

Fig. S6 TEM images of films made by depositing equal volume (10 µL) of EB solution of LM-P3HT (0.3 mg/mL) on the horizontal substrate followed by (a) removal of solvent under reduced pressure and (b) nitrogen flush at 25 ºC. Scale bar = 500 nm.

The solvent evaporation rate has a significant influence on the formation of P3HT nanowires. As Fig. S6 shows, amorphous granules or irregular aggregates instead of nanowire arrays are dominant on the film morphology except some short nanowires, when the thin liquid layer on the substrate was evacuated or blown with nitrogen gas instead of being placed in petri dish covered with a lid. With high evaporation rate of solvent, polymer chains failed to stack regularly into crystalline nanowires. In addition, the three-phase interface failed to recede gradually and evenly, resulting in isolated amorphous aggregates.

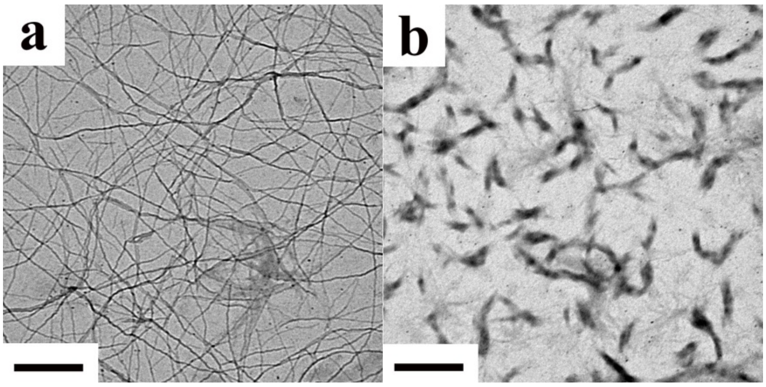

Fig. S7 TEM images of P3HT films made by depositing equal volume (10 µL) of EB solution (0.3 mg/mL) on the horizontal substrate at 25 ºC. The molecular weight of P3HT is (a) 2.0×10^4 g/mol and (b) 3.2×10^4 g/mol, respectively. Scale bar = 200 nm.

^{1}H NMR and SEC spectra of HM-P3HT sample

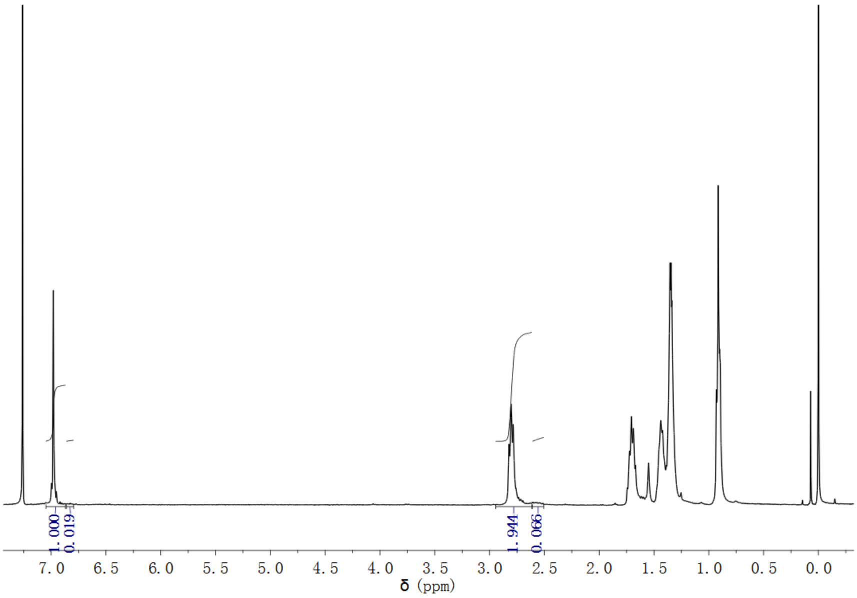

Fig. S8 ^{1}H NMR spectrum of HM-P3HT.

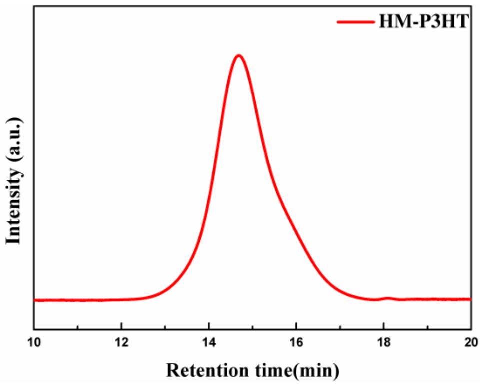

Fig. S9 Size exclusion chromatogram of HM-P3HT.

1D diffraction profile of GISAXS

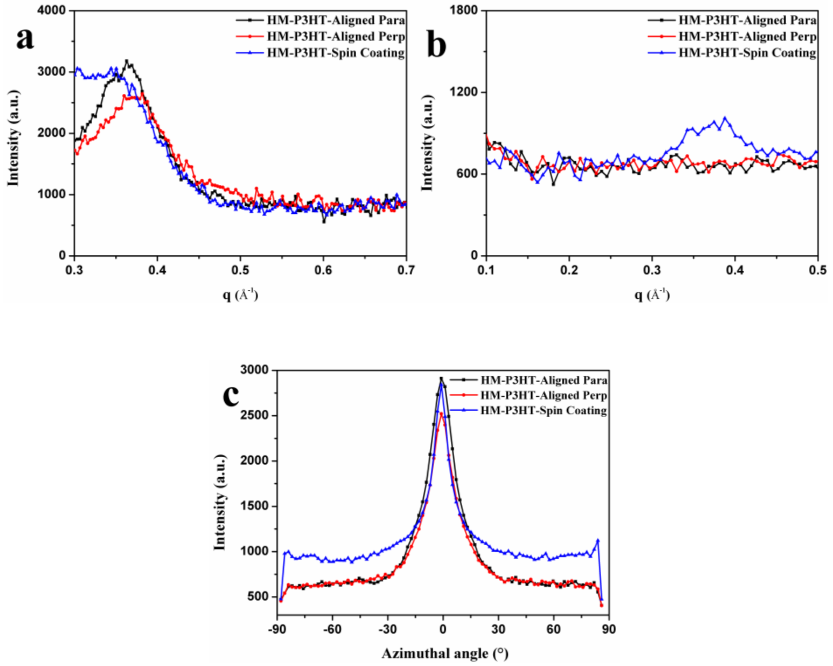

Fig. S10 1D diffraction profile with respect to the (a) out-of-plane cut (azimuthal angle = 0º, along q_z direction), (b) 45º cut (azimuthal angle = 45º, relative to q_z direction) and (c) azimuthal cut (intensity as a function of azimuthal angles) extracted from 2D-GISAXS patterns of Fig.6, respectively.

Mobility distribution of OFETs

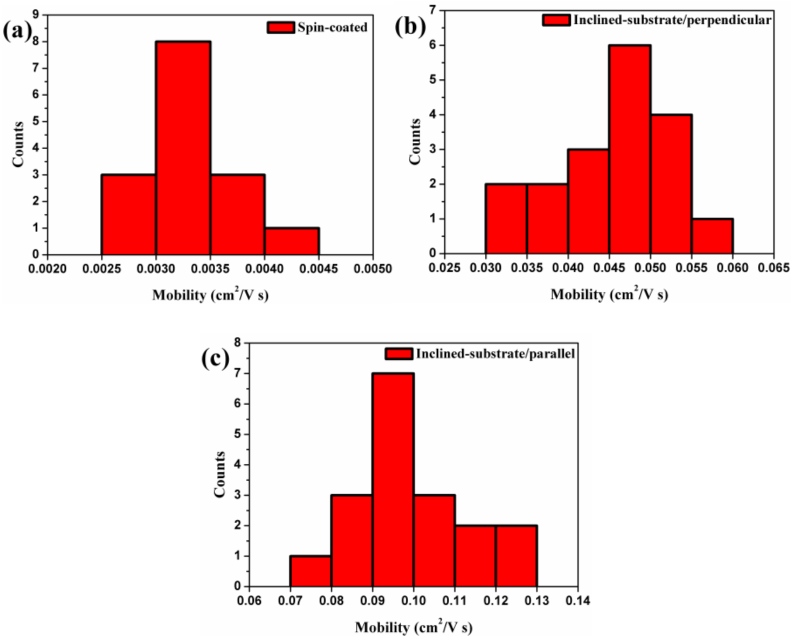

Fig. S11 Mobility distribution of OFETs with active layers (a) made by spin-coating method and made by inclined-substrate method with nanowire orientation (b) perpendicular and (c) parallel to the source-drain direction.

Reference

1 R. S. Loewe, S. M. Khersonsky and R. D. McCullough, *Adv. Mater.*, 1999, **11**, 250-253.
2 J. J. Richards, Ph.D., University of Washington, 2014.
3 C. M. Hansen, *Hansen solubility parameters: a user's handbook*, CRC press, 2007.
4 F. Machui and C. J. Brabec, *Semiconducting Polymer Composites: Principles, Morphologies, Properties and Applications*, 2012, 1-38.
5 T. Sato, S. Araki, M. Morimoto, R. Tanaka and H. Yamamoto, *Energy & Fuels*, 2014, **28**, 891-897.
6 M. Chang, D. Choi, B. Fu and E. Reichmanis, *ACS Nano*, 2013, **7**, 5402-5413.
7 X. N. Yang, *Semiconducting Polymer Composites: Principles, Morphologies, Properties and Applications*, John Wiley & Sons, 2012.
8 L. Bu, T. J. Dawson and R. C. Hayward, *ACS Nano*, 2015, **9**, 1878-1885.
9 Y. D. Park, S. G. Lee, H. S. Lee, D. Kwak, D. H. Lee and K. Cho, *J. Mater. Chem.*, 2011, **21**, 2338-2343.